

## COVER ARTICLE

# The light and hypoxia induced gene *ZmPORB1* determines tocopherol content in the maize kernel

Nannan Liu<sup>1,2†</sup>, Yuanhao Du<sup>1,2†</sup>, Shijuan Yan<sup>3</sup>, Wei Chen<sup>1,2</sup>, Min Deng<sup>4</sup>, Shutu Xu<sup>5</sup>, Hong Wang<sup>6</sup>, Wei Zhan<sup>7</sup>, Wenjie Huang<sup>3</sup>, Yan Yin<sup>8</sup>, Xiaohong Yang<sup>9</sup>, Qiao Zhao<sup>10</sup>, Alisdair R. Fernie<sup>11</sup> & Jianbing Yan<sup>1,2\*</sup>

<sup>1</sup>National Key Laboratory of Crop Genetic Improvement, Huazhong Agricultural University, Wuhan 430070, China;

<sup>2</sup>Hubei Hongshan Laboratory, Wuhan 430070, China;

<sup>3</sup>Agro-biological Gene Research Center, Guangdong Academy of Agricultural Sciences, Guangzhou 510640, China;

<sup>4</sup>College of Agronomy, Hunan Agricultural University, Changsha 410128, China;

<sup>5</sup>College of Agronomy, Northwest A&F University, Xi'an 710000, China;

<sup>6</sup>State Key Laboratory of North China Crop Improvement and Regulation, Hebei Sub-center of National Maize Improvement Center of China, College of Agronomy, Hebei Agricultural University, Baoding 071001, China;

<sup>7</sup>College of Life Sciences, South-Central Minzu University, Wuhan 430070, China;

<sup>8</sup>Plant Science Facility of the Institute of Botany, Chinese Academy of Sciences, Beijing 100093, China;

<sup>9</sup>National Maize Improvement Center of China, Beijing Key Laboratory of Crop Genetic Improvement, China Agricultural University, Beijing 100193, China;

<sup>10</sup>Shenzhen Key Laboratory of Synthetic Genomics, Guangdong Provincial Key Laboratory of Synthetic Genomics, Shenzhen Institute of Synthetic Biology, Shenzhen Institute of Advanced Technology, Chinese Academy of Sciences, Shenzhen 518055, China;

<sup>11</sup>Max Planck Institute of Molecular Plant Physiology, Potsdam-Golm 14476, Germany

†Contributed equally to this work

\*Corresponding author (email: [yjianbing@mail.hzau.edu.cn](mailto:yjianbing@mail.hzau.edu.cn))

Received 10 August 2023; Accepted 11 November 2023; Published online 18 January 2024

**Tocopherol is an important lipid-soluble antioxidant beneficial for both human health and plant growth. Here, we fine mapped a major QTL-*qVE1* affecting  $\gamma$ -tocopherol content in maize kernel, positionally cloned and confirmed the underlying gene *ZmPORB1* (*por1*), as a protochlorophyllide oxidoreductase. A 13.7 kb insertion reduced the tocopherol and chlorophyll content, and the photosynthetic activity by repressing *ZmPORB1* expression in embryos of NIL-K22, but did not affect the levels of the tocopherol precursors HGA (homogentisic acid) and PMP (phytyl monophosphate). Furthermore, *ZmPORB1* is inducible by low oxygen and light, thereby involved in the hypoxia response in developing embryos. Concurrent with natural hypoxia in embryos, the redox state has been changed with NO increasing and H<sub>2</sub>O<sub>2</sub> decreasing, which lowered  $\gamma$ -tocopherol content via scavenging reactive nitrogen species. In conclusion, we proposed that the lower light-harvesting chlorophyll content weakened embryo photosynthesis, leading to fewer oxygen supplies and consequently diverse hypoxic responses including an elevated  $\gamma$ -tocopherol consumption. Our findings shed light on the mechanism for fine-tuning endogenous oxygen concentration in the maize embryo through a novel feedback pathway involving the light and low oxygen regulation of *ZmPORB1* expression and chlorophyll content.**

maize | tocopherol | hypoxia | photosynthesis | *ZmPORB1* |

## INTRODUCTION

Tocopherol is a fatty-acid soluble antioxidant. Tocopherol synthesis occurs in the plastids of photosynthetic organisms, but is absent in humans and animals rendering it an important dietary component (Fitzpatrick et al., 2012). The pathway of tocopherol biosynthesis is generally conserved across high plants and photosynthetic bacteria (Sattler et al., 2003), and several key genes controlling the synthesis of tocopherol in the model plant *Arabidopsis* and maize have been described (Albert et al., 2022; Diepenbrock et al., 2017; Fiedler et al., 1982; Fritsche et al., 2017; Soll et al., 1980). Phytyl diphosphate (PDP), the source of saturated isoprenoid side chain of tocopherol, is condensed with HGA, the precursor of the aromatic ring, which is the key step affecting the total tocopherol content (Collakova and DellaPenna, 2003). In addition, phytol from chlorophyll degradation can be phosphorylated twice to form PMP and PDP,

which also take part in tocopherol synthesis (Valentin et al., 2006; vom Dorp et al., 2015). Recently, a large-scale QTL study in NAM populations has identified many loci affecting tocopherol content in maize kernel, and two homologous maize genes, *por1* and *por2*, annotated as light-dependent protochlorophyllide oxidoreductases, were nominated to affect the tocopherol content displaying a positive relationship with chlorophyll content in maize embryos (Diepenbrock et al., 2017). Later, *por2* was validated genetically to play a role mainly in leaves (Zhan et al., 2019). This may occur via a mechanism in which phytol levels are altered as a result of chlorophyll degradation despite the fact that the chlorophyll levels are about 800 times lower than tocopherol levels in the embryos (Diepenbrock et al., 2017).

Tocopherol exists in diverse tissues of higher plants (Horvath et al., 2006). Generally speaking,  $\alpha$ -tocopherol is dominant in leaves, but in roots, stems, fruits and seeds,  $\gamma$ -tocopherol is the

most prevalent form. In maize kernels, most tocopherol accumulates in the embryos (Rocheford et al., 2002). Tocopherols are of benefit to seed dormancy, longevity and dehydration as well as in improving the resistance of plants to high light, temperature, salt and microbial pathogens (Abbasi et al., 2007; Maeda et al., 2005; Maeda et al., 2006; Mène-Saffrané and DellaPenna, 2010; Munné-Bosch, 2005; Sattler et al., 2004; Stahl et al., 2019).  $\gamma$ -tocopherol, in particular, is important for scavenging reactive nitrogen species (RNS) by means of a nitration reaction involving the free methyl group of the fifth carbon (Christen et al., 1997; Cooney et al., 1993). In plants, it was reported that  $\gamma$ -tocopherol controlled seed germination by regulating nitric oxide (NO) content in this manner (Desel et al., 2007; Desel and Krupinska, 2005), which seems to be linked with enrichment of  $\gamma$ -tocopherol in plant seeds.

In developing maize seeds, the average steady-state oxygen concentration is some 15% of that generally found in the atmosphere, i.e., in the low oxygen range (Borisjuk et al., 2007; Rolletschek et al., 2005). The oxygen content inside the developmental seeds is determined by the diffusion from the ambient atmosphere, and the generation of oxygen by seed photosynthesis (Borisjuk and Rolletschek, 2009). However, the pericarp covering the seeds, alongside the attached seed coat and the lipid-rich membrane covering the embryo tend to block oxygen diffusion. Besides, the active respiratory metabolism of some tissues such as the developmental embryo will additionally consume considerable amounts of oxygen, which will, in turn, exacerbate the oxygen shortage. For this reason, plants sense hypoxia and adaptatively respond via diverse pathways including a restraint of respiration and a consequent decrease of ATP consumption resulting from the inhibition of a large-scale of biosynthetic processes. They moreover enhance endogenous levels of NO to improve oxygen availability, the involvement of antioxidants and the molecular regulation of genes at the transcriptional and posttranscriptional levels (Blokhina and Fagerstedt, 2010; Geigenberger, 2003; Pucciariello and Perata, 2017; van Dongen and Licausi, 2015; Weits et al., 2021). Among these, NO is a pivotal regulator which is triggered by hypoxia and decreases on sensing elevated oxygen (Borisjuk et al., 2007). Therefore, it is likely that  $\gamma$ -tocopherol takes part in the hypoxic response in aiming to maintain the redox balance.

The photosynthetic activity of seeds, by contrast to that of respiration, alleviates oxygen limitations. In seeds having a green pericarp such as wheat or a green embryo such as legume seeds, the oxygen level inside the embryo is dramatically affected by lighting conditions due to the operation of photosynthesis (Borisjuk et al., 2007; Borisjuk and Rolletschek, 2009). In a recent study, chlorophyll was detected in the maize embryo but not the endosperm, and found to gradually decrease on kernel maturation (Diepenbrock et al., 2017). As such, whether maize embryo containing chlorophyll performs photosynthesis or not remains unclear.

In the current study, we cloned and reverse genetically validated a major QTL-*qVE1* for tocopherol content of maize kernels, and further clarified the function of tocopherol in developing maize embryo, providing new insights into maize kernel metabolism which we believe will facilitate breeding of maize of high-nutritional value.

## RESULTS

### Fine mapping of the major QTL-*qVE1* controlling the content of tocopherol in maize grain

A major QTL, *qVE1*, affecting  $\gamma$ -tocopherol,  $\alpha$ -tocopherol and their two derivative traits—total tocopherol and ratio of  $\alpha$ - to  $\gamma$ -tocopherol—explaining up to 33.5% of phenotypic variation for  $\gamma$ -tocopherol, was identified in a DAN340/K22 recombinant inbred line (RIL) population (Figure 1A). One heterogeneous inbred family (HIF) was used to validate the QTL by progeny tests, revealing that  $\gamma$ -tocopherol (Student's *t*-test,  $P=8.3\times 10^{-4}$ ) and total tocopherol ( $P=1.3\times 10^{-4}$ ) were significantly different between the two parental homozygotes NIL-DAN340 and NIL-K22 (Figure 1B; Table S1 in Supporting Information), while  $\alpha$ -tocopherol and ratio of  $\alpha$ - to  $\gamma$ -tocopherol were not significantly altered (Table S1 in Supporting Information). To fine map *qVE1*, five recombinants, R1 to R5, derived from the HIF line within the 2.3 Mb QTL interval were used to narrow the QTL to a 26 kb interval spanning chr1: 227,508,000–227,534,000, flanked by M6 and M10 (Figure 1C). A single gene *GRMZM2G036455*, likely corresponding to *ZmPORB1* was located in this region on the basis of the B73 reference genome (RefGen\_V2). It was annotated as a light-dependent NADPH: protochlorophyllide oxidoreductase playing an important role in the biosynthesis of chlorophyll by catalyzing the conversion of protochlorophyllide a to chlorophyllide a (Figure 1D). Among them, the recombination breakpoints of two recombinants (R4–R5) were located between the second and third exons of *ZmPORB1*, indicating that the two regions differentiating M6–M8, M8 and M10 both contained causal variants of *ZmPORB1* (Figure 1C and D). Based on the sequence of *qVE1*-containing BAC clones of K22, it showed 13.7 kb transposon insertion was present in the promoter of candidate gene *ZmPORB1* of K22 within the 26 kb candidate region (Figure 1D).

### 13.7 kb transposon-related insertion and a nonsynonymous mutation are putative causal polymorphic variations

In order to uncover the causative variants of the candidate gene *ZmPORB1* between K22 and DAN340, we subsequently identified a total of 214 polymorphic sites spanning more than 1 kb upstream of transcription start sites (TSS) of *ZmPORB1* to 3'-untranslated region (UTR), which were used to perform candidate gene association analysis in a maize association mapping panel (AMP) containing 513 maize inbred lines (Figure 2A; Yang et al., 2011). Two polymorphic sites were significantly associated with the contents of tocopherol: the 13.7 kb transposon-related presence and absence variation (PAV) in the promoter region, which explained 2.3% of total tocopherol variation ( $N=414/28$ ,  $P=1.6\times 10^{-3}$ ) and a nonsynonymous SNP variation in the fourth exon (C-G, Arg-Gly) which explained 4.2% of total tocopherol variation ( $N=171/153$ ,  $P=1.9\times 10^{-5}$ ) (Figure 2A–C). *ZmPORB1* haplotypes were next used to estimate the joint effects of 13.7 kb PAV and C/G SNP on total tocopherol content, only three haplotypes were observed which could explain 8.2% of the phenotypic variation in AMP (Figure 2D). Of all three observed haplotype classes, total tocopherol content was highest when the favorable alleles of 13.7 kb PAV (absent) and C/G SNP (G/G) were combined (DAN340 type), being 50%

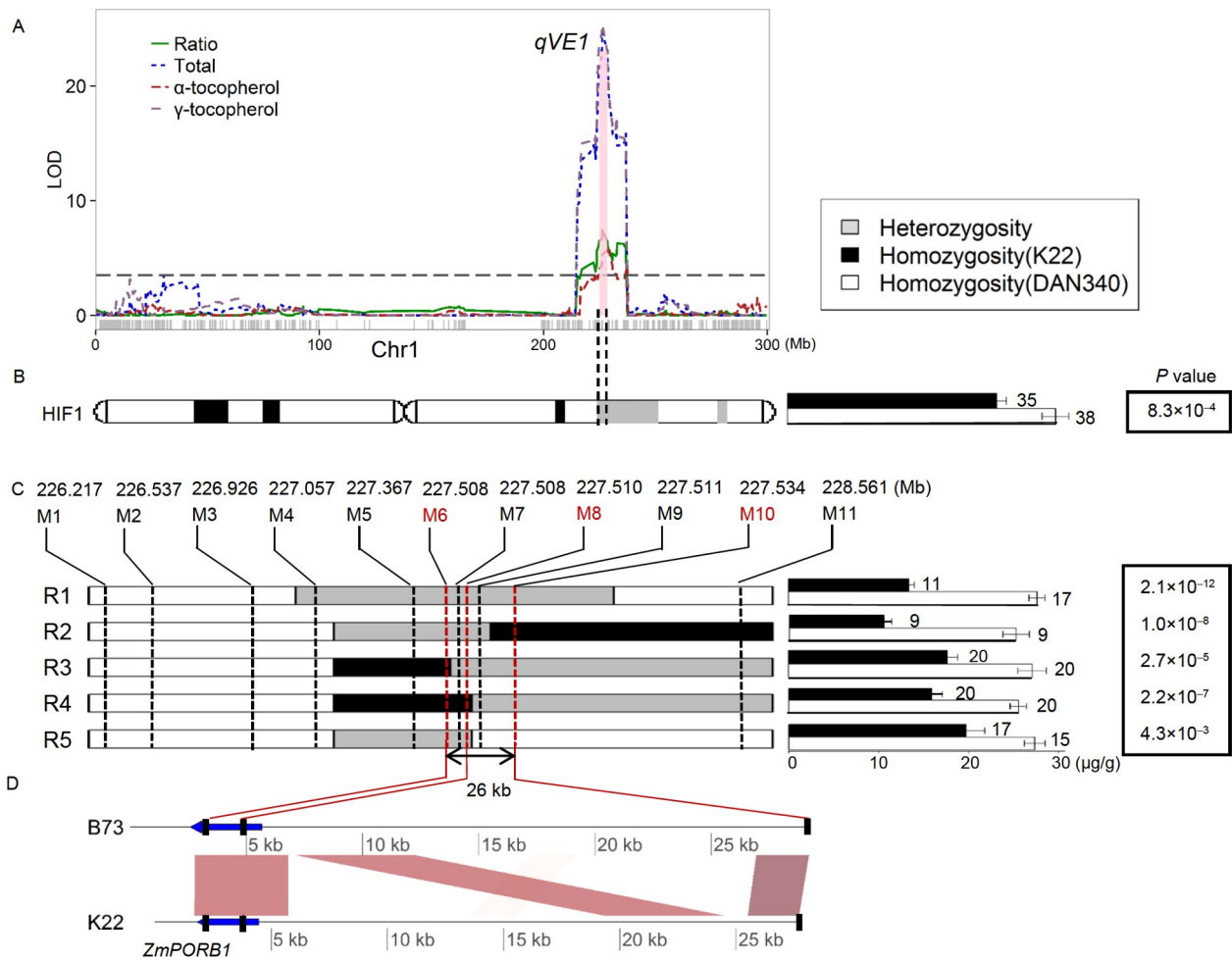


**Figure 1.** Fine mapping of *qVE1*. A. QTL mapping of four tocopherol-related traits in mature maize kernels. The LOD cutoff was set at 3.5 by 500 permutations. Ratio:  $\alpha$ - to  $\gamma$ -tocopherol, Total: sum of  $\alpha$ - and  $\gamma$ -tocopherol. B. Validation of *qVE1* by progeny tests from one HIF (heterogeneous inbred lines family) that was heterozygous in *qVE1* region and homozygous in the most other regions. C. The further fine mapping of *qVE1* using 5 HIF-derived recombinants: R1–R5 and progeny tests. The white and black bars indicate chromosomal segments from DAN340 or K22 parent, respectively, in *qVE1* confidence intervals. The numbers and text above all of the bars represent the physical locations (Mb) and names of markers. The names of the recombinants are on the left of bars and on the right of bars, the corresponding content of  $\gamma$ -tocopherol of two genotype groups (white: DAN340 type, black: K22 type) are shown (mean $\pm$ SE). The numbers of samples measured and the *P*-values of one-way ANOVA between the near-isogenic lines (NILs) are shown on the right of phenotype bars. D. The collinear genomic regions covering the 26 kb candidate regions of B73 and K22 BAC sequences are represented by pink shading, and the predicted genes including *ZmPORB1* are depicted by blue arrows. The black lines designate the markers M6, M8 and M10 flanking the 26 kb candidate region.

higher than the level documented for the least favorable haplotype class (K22 type; Figure 2D).

### 13.7 kb PAV affects tocopherol content by regulating the expression level of *ZmPORB1*

Amongst 23 maize tissues investigated within the B73 genotype, the levels of *ZmPORB1* mRNA are high in the embryo and mature leaf and intermediate in the endosperm crown and pericarp (Walley et al., 2016). In order to verify the expression pattern, mature leaf, developing embryo, and endosperm at 10 days after pollination (DAP), 15 DAP, 25 DAP and 30 DAP were collected from the near-isogenic lines (NIL-DAN340 and NIL-K22). As expected, *ZmPORB1* mRNA levels were high in the embryo and mature leaf and low in the endosperm (Figure 3A; Figure S1A in Supporting Information). In the developing embryo, *ZmPORB1* exhibited peak expression at 10 DAP with expression subsequently decreasing significantly at 15, 25 and

30 DAP. Significant differences in gene expression levels between NIL-DAN340 and NIL-K22 were observed throughout embryo development (Figure 3A). However, the general expression levels observed in the leaf were similar in both genotypes (Figure 3A). Collectively, these results thus suggest that influencing the expression of *ZmPORB1* results in tissue and development stage-specific effects.

Based on the RNA sequencing data of the immature kernels at 15 DAP in 368 maize inbred lines (Fu et al., 2013), we found that *ZmPORB1* expression level was significantly correlated with total tocopherol content ( $r=0.24$ ,  $P=2.6\times 10^{-5}$ ). Consistent with this global analysis, the lines harboring the 13.7 kb TE insertion displayed both lower total tocopherol content and lower *ZmPORB1* expression with the latter being at 25% of the level found in the controls ( $N=20/220$ ,  $P=1.5\times 10^{-9}$ ) (Figure 3B and C). This observation was confirmed in the segregating progenies of recombinants R4 within *ZmPORB1*, the progenies with the DAN340 genotype in the promoter from R4 showed significantly

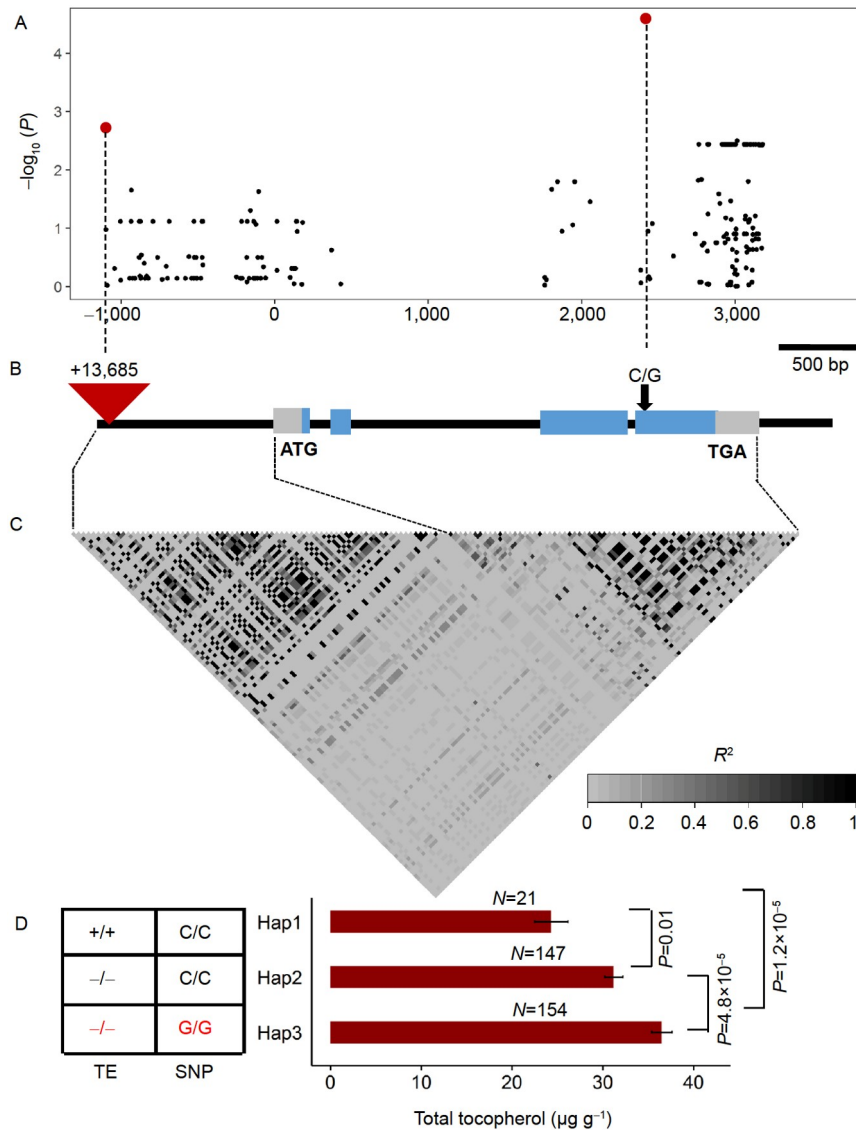


**Figure 2.** The 13.7 kb PAV and nonsynonymous SNP located in *ZmPORB1* associated with total tocopherol variation. A, Association signals ( $-\log_{10}P$ -values (ANOVA)) for total tocopherol of 214 polymorphic sites across  $\sim 4$  kb of *ZmPORB1*. The two red points correspond to 13.7 kb TE-PAV and nonsynonymous SNP. B, The map of *ZmPORB1* with major structure variations between K22 and DAN340. The grey boxes indicate the UTR, the blue boxes represent the exons, and the triangles indicate the insertions of transposons of different sizes. The two significant polymorphic sites in the promoter and the fourth exon are designated with black lines. C, The linkage disequilibrium (LD) blocks across the  $\sim 4$  kb of *ZmPORB1*. D, The only three haplotypes of the two relevant polymorphic sites and the corresponding total tocopherol content are shown (mean $\pm$ SE). The Hap1 was the K22 type, and the Hap 3 (DAN340 type) marked red has no TE insertion and G/G SNP was most favorable (one-way ANOVA).

higher expression and tocopherol content than those harboring the K22 genotype (Figure 1C; Figure S1B in Supporting Information). The implication of these studies is that total tocopherol content can be elevated by increasing the expression level of *ZmPORB1*. In order to validate this hypothesis, we obtained two independent overexpression lines (OE1 and OE2) containing the DAN340-type coding region sequence of *ZmPORB1* driven by *ZmUbi* promoter. The *ZmPORB1* expression levels significantly increased in  $T_3$  transgenic lines compared to the control in segregating progenies from OE1 and OE2 ( $N=18/21$ ,  $P=6.7\times 10^{-3}$ ;  $N=17/17$ ,  $P=3.8\times 10^{-5}$ ). Accordingly,  $\gamma$ -tocopherol content in maize grain was significantly enhanced in these overexpression lines in both families ( $N=18/20$ ,  $P=9.3\times 10^{-3}$ ;  $N=14/19$ ,  $P=1.2\times 10^{-3}$ ) (Figure 3D). Additionally, we detected that  $\gamma$ -tocopherol decreased in knock-out lines compared with the negative control in segregating progenies

from two independent knockout lines ( $N=9/11$ ,  $P=9.7\times 10^{-3}$ ;  $N=18/29$ ,  $P=4.2\times 10^{-3}$ ) (Figure 3E; Figure S2C in Supporting Information).

### ***ZmPORB1* affected the chlorophyll content in maize kernel but not in leaf**

Phylogenetic analysis of *ZmPORB1* homologs in maize, rice, sorghum, *Brachypodium* and *Arabidopsis* revealed that the two paralogs *ZmPORB1* and *ZmPORB2* clustered together, suggesting that they arose by genome duplication (Figure S3A in Supporting Information). All homologous genes have the light-dependent protochlorophyllide oxidoreductase domain (Figure S3B in Supporting Information). However, compared with the other genes which expressed mainly in leaves and shoots, *ZmPORB1* most highly expressed in the embryos and leaves

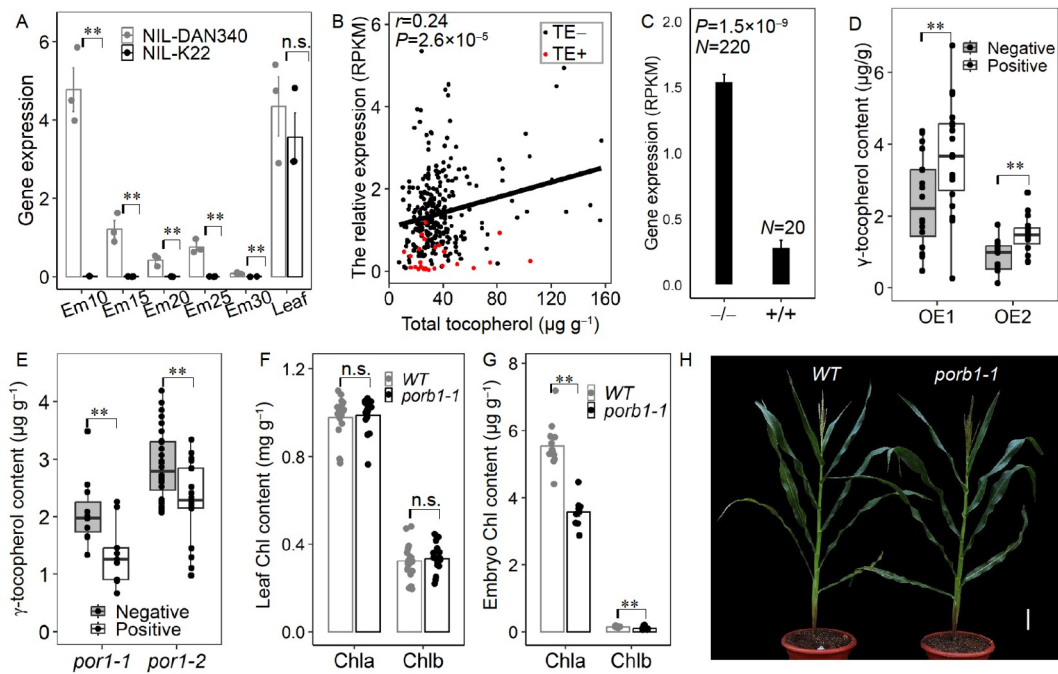


**Figure 3.** The relationship of 13.7 kb TE PAV, the expression level of *ZmPORB1* in embryos, and total tocopherol content in kernels. A, *ZmPORB1* expression in embryos at 10, 15, 25, 30 DAP and in mature leaves from two NILs of K22 and DAN340. B, The correlation between *ZmPORB1* expression and content of total tocopherol in AMP (368 lines). Red dots represent the lines with 13.7 kb TE insertion and black dots represent the lines without 13.7 kb TE insertion. C, The 13.7 kb TE PAV significantly affected the *ZmPORB1* expression in AMP. D and E, The comparison of the  $\gamma$ -tocopherol content in mature kernels between lines of transgenic genotype and those of non-transgenic genotype within four families from two overexpression events OE1, OE2 and two knockout events. F and G, *por1-1* had no effect on the chlorophyll in leaves (fresh weight), but significantly affected the chlorophyll a and b in developing embryos (dry weight). H, The agronomic traits of the knockout lines of *porb1-1*. Bar=10 cm. Data was mean $\pm$ SE; \*,  $P<0.05$ ; \*\*,  $P<0.01$ ; n.s., not significant (one-way ANOVA).

(Figure S3C in Supporting Information).

Subcellular localization experiments indicated that the *ZmPORB1* protein was targeted to the chloroplast of maize protoplasts (Figure S2A in Supporting Information). The knockout lines displayed significantly decreased chlorophyll contents in embryos but not in leaves, which furthermore showed no obvious morphological changes under normal growth conditions (Figure 3F–H). *ZmPORB1* displayed an epistatic interaction with its paralog *ZmPORB2* for  $\gamma$ -tocopherol contents (Diepenbrock et al., 2017), which meant that under the background of weak mutations in *ZmPORB2*, the weak mutations of *ZmPORB1* exhibited significant phenotype difference. Under normal conditions of *ZmPORB2*, *ZmPORB1* mutations displayed almost no phenotypic differences (Figure S2B in Supporting Information). Therefore, we first verified that knockout lines of *ZmPORB2* have etiolated leaves and a notably delayed development (Figure S2D and E in Supporting Information). As would perhaps be expected the chlorophyll content in leaves of the knockout lines was heavily decreased, while the tocopherol content was elevated in leaves but decreased in the kernels (Figure S2F–H in Supporting Information). Furthermore, the *porb1-2/porb2* double mutant showed severe developmental defects with no kernels, whilst the chlorophyll content in leaves was heavily decreased, and the tocopherol content of this tissue was significantly elevated (Figure S2F and G in Supporting Information).

It has been reported that the phytol from chlorophyll degradation can be converted to phytol monophosphate (PMP) and phytol diphosphate (PDP) with these products serving as substrate of tocopherol synthesis (Valentin et al., 2006; vom Dorp et al., 2015). If *ZmPORB1* directly regulates the tocopherol

content in maize kernels via the chlorophyll pathway, it follows that the PMP or PDP content should be different between the NILs. However, there was no difference in PMP levels between the NILs in mature kernels ( $N=4/7$ ,  $P=0.6$ ) or developing kernels at 25, 30 and 35 DAP (Figure S4A and B in Supporting Information). Furthermore, there was also no difference in the levels of the other key precursor, HGA, between the NILs ( $N=7/7$ ,  $P=0.8$ ) (Figure S4B in Supporting Information), indicating that the observed variation of tocopherols in kernels is not due to the change in flux of chlorophyll and tocopherol synthesis and may rather be related to differences in tocopherol degradation.

In mature leaves, the  $\alpha$ -tocopherol level was 10 times higher than that of  $\gamma$ -tocopherol—yet both were invariant between the NILs ( $N=3/3$ ,  $P=0.8$ ). In the kernels, however,  $\gamma$ -tocopherol was dominant and the differences in its levels between the two NILs became ever greater throughout its accumulation (Figure S4C and D in Supporting Information). These results thus indicate that the difference in  $\gamma$ -tocopherol level of kernels was due to the differential *ZmPORB1* expression in the embryo itself, and not a consequence of altered tocopherol metabolism in the leaves. The question remained, however, as to the mechanism by which *ZmPORB1* impacts  $\gamma$ -tocopherol content via the chlorophyll content of the maize kernels?

### *ZmPORB1* is involved in hypoxia response in maize kernels

We predicted several light-responsive elements and one regulatory element for anaerobic induction in the promoter of *ZmPORB1*. Therefore, we subsequently found that *ZmPORB1* expression in 15 DAP kernel of NIL-DAN340 significantly

increased by more than 2-fold both in hypoxic and anaerobic conditions, while the expression in NIL-K22 significantly elevated only in the anaerobic condition (Figure 4A). These results meant that *ZmPORB1* was induced by low oxygen and that the K22 genotype had decreased sensitivity for oxygen response in maize kernels. It is also noteworthy that the expression of *ZmPORB1* in developing kernels was significantly induced by blue and red light in the DAN340 genotype. However, as was the case with the oxygen response, the sensitivity of the light response was lost in the maize kernels of the K22 genotype (Figure 4A).

We next identified common differently expressed genes (DEGs) between the embryos of two NILs at 10, 15 and 25 DAP and embryos of NIL-DAN340 treated with low oxygen. In total, 8.4%, 10.4% and 22.2% of genes that were differently expressed in the three stages of developing embryos were shared with those of the hypoxic embryos (Figure 4B; Dataset S1 in Supporting Information). The up-regulated DEGs of both developing and hypoxic embryos were enriched in energy metabolism, encompassing the glycolytic process, pyruvate metabolism and ATP generation (Figure S5A–C and Dataset S2 in Supporting Information). It is important to note that six DEGs across the three developing stages were shared with the 49 core genes previously observed to transcriptionally respond to low oxygen in shoots and roots of plants (Table S2 in Supporting Information, Mustroph et al., 2010). The homolog of one of the crucial genes, GRMZM2G316362, annotated as stearyl-acyl-carrier-protein desaturase 9 responsible for oleic acid biosynthesis, was reported to be induced by hypoxia (Klinkenberg et al., 2014). Yet no known chlorophyll and tocopherol pathway related genes were found to be differently expressed here (Dataset S3 in Supporting Information). That said, several lines of evidence suggest that *ZmPORB1* participates in the response pathway to naturally occurring hypoxic-stress within the developing embryos.

Another downregulated hub gene GRMZM2G067402—encodes a non-symbiotic hemoglobin 1, which is known to catalyze the oxidation of nitric oxide (NO) to nitrate during hypoxic conditions (Table S2 in Supporting Information). NO levels are regulated to promote oxygen availability as an essential adaptive response to balance oxygen and ATP availability in hypoxic plant tissues (Borisjuk et al., 2007). In keeping with this, we found that the NO content was prominently increased in 15DAP embryos of NIL-K22 (Figure 4C), but that ROS and hydrogen peroxide ( $H_2O_2$ ) levels were significantly lower (Figure S6A and B in Supporting Information). These findings hint that more serious hypoxia led to redox changes such that NO levels accumulated and lower  $H_2O_2$  production occurred in embryos of NIL-K22. Additionally, the  $\gamma$ -tocopherol contents of kernels in both of the two NILs decreased under NO donor treatment (sodium nitroprusside) with a greater change in NIL-K22, while increased following  $10\text{ mmol L}^{-1} H_2O_2$  treatment with a greater change in NIL-DAN340 (Figure 4D). That said,  $\gamma$ -tocopherol reacted to the increasing NO resulting from hypoxia and the different extents of response confirmed the distinct endogenous redox poise of the two NILs.

We assumed that the hypoxic response was associated with embryo photosynthesis by controlling chlorophyll content from the regulation of *ZmPORB1* expression under light and oxygen cues. As expected, the developing embryos of NIL-DAN340 with more chlorophyll showed higher minimum chlorophyll fluorescence under dark adapted states and effective quantum yield of

photosystem II under light stable states using a micro chlorophyll fluorometer (Figure 5A–D). This observation underlined that the developing maize embryo was photosynthetically active, and affected by chlorophyll content although this activity was admittedly relatively weak.

## Light and hypoxia responsive elements in the promoter of *ZmPORB1*

*ZmPORB1* expression was strongly induced by light and hypoxia in the maize embryos, suggesting that its promoter may have cis-elements for the light and hypoxia response. Since the 13.7 kb insertion decreased the *ZmPORB1* expression located in the 1.25 kb upstream of start codon, we first performed transient dual-luciferase reporter assays to compare the activity of 1.5 or 1.25 kb of the DAN340 allele and 1.25 kb of the K22 allele of *ZmPORB1* in maize protoplasts (Figure S7A in Supporting Information). There was no difference between DAN340 and K22 allele 1.25 kb promoters, confirming that the DNA variations located in this region do not affect the gene expression. By contrast, the transcriptional activity of the 1.5 kb region was slightly higher (1.16 folds change) than the 1.25 kb of the DAN340 allele (Figure S7A in Supporting Information), which means that the 13.7 kb insertion seems to disrupt *ZmPORB1* expression by DNA modification rather than the destruction of the cis-element sequences themselves. To further identify the light and hypoxia responsive cis-elements, we detected the activity of series of truncated promoters in the 1.25 kb range, and discovered four suppressive regions, consisting of R1, R3, D255\_310, D718\_1250 (Figure 6A; and Figure S7A in Supporting Information) and one activated region R2, which was verified by transient expression of these five fragments within the minimal promoter (Figure 6B; Figure S7B in Supporting Information). Furthermore, we found that the transcriptional activities of both R1 and R3 regions were provoked by blue light, while R1 was additionally induced by red light (Figure 6C). Similarly, the transcriptional activity of R2 was induced by hypoxia (Figure 6D). These results demonstrate that the light and hypoxia responsive cis-elements underlay the corresponding responses of the developing maize embryos.

Combining the above findings, we propose a model as to how *ZmPORB1* is involved in hypoxic and light responses to affect chlorophyll, NO, and  $\gamma$ -tocopherol levels in the developing maize embryos (Figure 6E). During kernel development, *ZmPORB1* expression is regulated by incident light approaching the embryo surface and low oxygen, and further affects chlorophyll synthesis, which consequently influences photosynthetic activity and oxygen release to relieve the extreme oxygen deprivation observed in this tissue. Meanwhile,  $\gamma$ -tocopherol reacts to the promoted NO responding to hypoxia, which leads to its consumption and content variation. We postulate an elaborate regulation by which plants control chlorophyll content by fine-tuning *ZmPORB1* expression to sustain the oxygen homeostasis in maize developing embryo.

## DISCUSSION

### *ZmPORB1* controls the content of tocopherol in maize kernel

Here, we cloned the relevant allelic variants of *ZmPORB1* gene

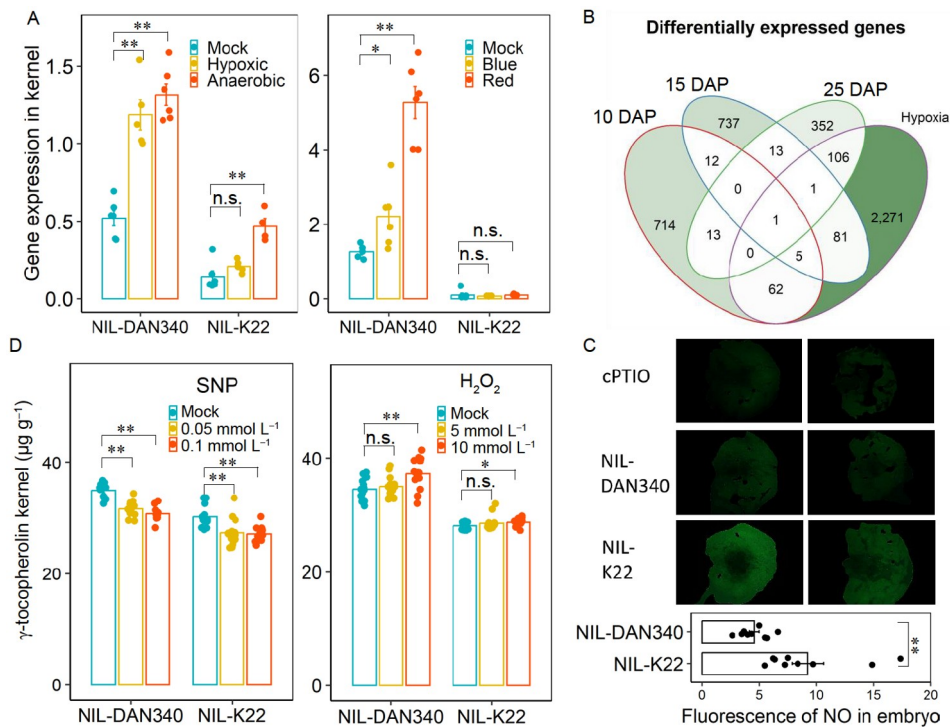


**Figure 4.** *ZmPORB1* participated in regulation of oxygen content in maize embryos. A, Effect of light (red and blue light) and oxygen stress (hypoxic and anaerobic) on *ZmPORB1* expression in embryos of NIL-DAN340 and NIL-K22. B, Venn diagrams summarizing the number of DEGs contrasting the developing embryos (10, 15, 25 DAP) of the two NILs and hypoxia-treated embryos of NIL-DAN340. C, The nitric oxide content in 15 DAP embryos of NIL-DAN340 and NIL-K22 quantified by the fluorescence intensity reacting with DAF-FM DA. Two biological repeats were shown. cPTIO (carboxy-PTIO) is the NO scavenger as the negative control. D, The  $\gamma$ -tocopherol content in 25 DAP kernels by the treatments of two concentration gradients of NO donor (sodium nitroprusside) and hydrogen peroxide. Data was mean $\pm$ SE; \*,  $P < 0.05$ ; \*\*,  $P < 0.01$ ; n.s., not significant (one-way ANOVA).

and used reverse genetics to confirm that it controls total and  $\gamma$ -tocopherol content in the maize kernel. A 13.7 kb TE-related PAV in the promoter and a coding SNP resulting in an arginine to glycine transformation were statistically identified as candidate causal variants. The 13.7 kb insertion decreases the content of tocopherol and the transcription level of *ZmPORB1* by genetic analysis, whilst the causal SNP may affect either the protein function or enzyme activity, but until now, we have no genetic evidence to verify this and further experiments such as base-editing will be required to define the exact effects underlying the observed phenotypes.

### The regulation of *ZmPORB1* expression may be an adaptive response to the environments of multiple tissues or biological processes

Both our results and previous studies showed that chlorophyll a and b were detected in the developing embryos, although it was at least 150 times less (dry weight /fresh weight) than those in leaves, inferring that light can penetrate the pericarp, seed coats and embryo. Meanwhile, at the transcriptional level, *ZmPORB1* responded to light in leaves, which was similar to that of the K22 genotype, although the response sensitivity was reduced especially for red light (Figure S8A and B in Supporting Information). For the K22 genotype (harboring the 13.7 kb TE insertion), the much severer reduction of embryo responsiveness to light and hypoxia explained the pattern that *ZmPORB1* expression was normal in leaves, but negligible in the embryo (Figure 3A). Interestingly, we observed a similar pattern of

*ZmPORB1* expression in the innermost and outermost layers of maize bracts with the lowest and highest chlorophyll, respectively (Figure S8C in Supporting Information). Unlike this situation, *ZmPORB1* expression was not affected by the 13.7 kb TE insertion in outermost bracts and leaves, but was significantly diminished by three times in the innermost bracts compared with the NIL-DAN340 genotype (Figure S8C in Supporting Information). Thus, based on several lines of evidence, we believe that the tissue-specific light-response of *ZmPORB1* is related to the distinct intensity of light absorption across diverse tissues, containing leaves, multiple layers of bracts and embryos.

The question arises why the 13.7 kb insertion has a stronger effect on *ZmPORB1* expression in embryos and the innermost bracts. Tissue-specific microenvironments clearly result in variance in *ZmPORB1* expression. For leaves and the outermost bracts, sufficient absorbance of sunlight compensated for the impairment in the response to light caused by the 13.7 kb TE insertion. However, for embryos and innermost bracts, the reduced tissue penetrance of light led to the reduction of *ZmPORB1* expression and consequently a reduced chlorophyll synthesis. This decrease was exacerbated by the 13.7 kb TE insertion. Whereas, the oxygen response was specific for the tissues such as the embryos that were subject to hypoxia. From the perspective of DNA methylation, we observed that the pattern of CHH methylation was more extensive and distinct across the promoter compared with those of CG and CHG types (Figure S9A and B in Supporting Information). The 13.7 kb TE insertion modifies the CHH type of *ZmPORB1* DNA methylation in the two light-responsive and one hypoxia-responsive elements of the

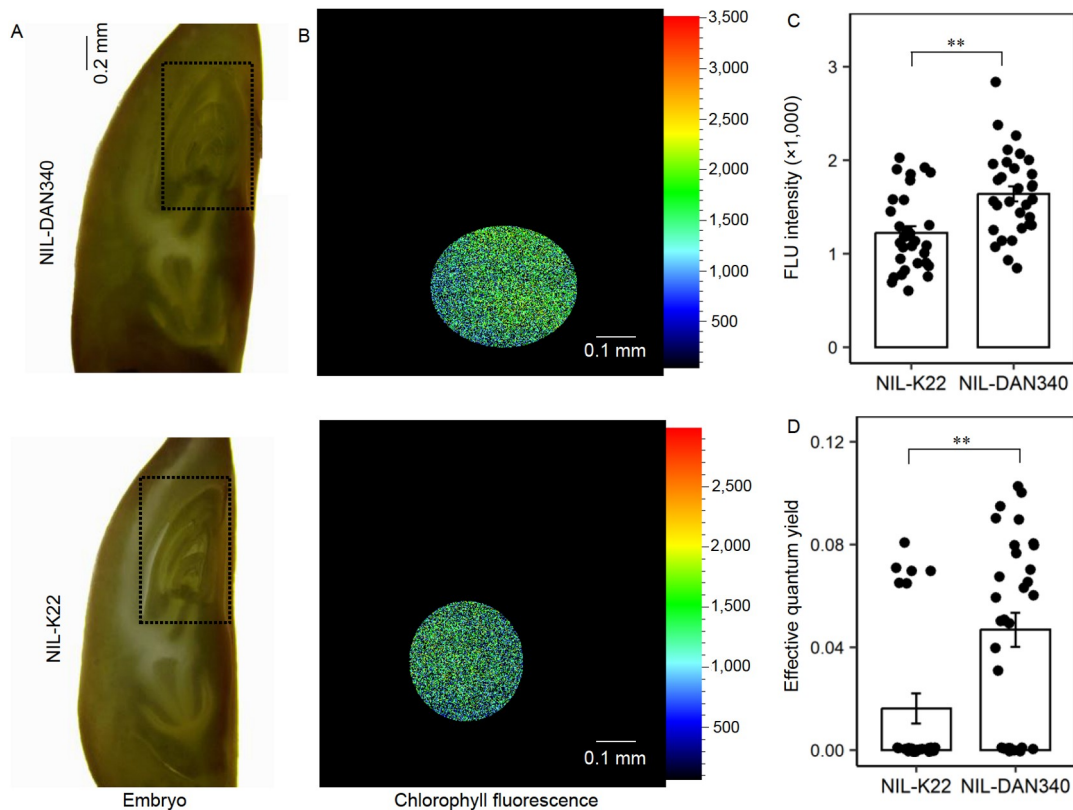


**Figure 5.** Photosynthesis in the maize embryo. A, Longitudinal section of embryos at 17 DAP of the two NILs. The plumule of embryos in the dashed box was used to measure the chlorophyll fluorescence at the adapted dark and light. B, The minimum chlorophyll fluorescence of plumule of embryos at dark-adapted state. The scale shows the relationship between the color and fluorescence. C, The comparison of minimum chlorophyll fluorescence of the 17 DAP plumule from dark-adapted state between the two NILs. D, The comparison of effective quantum yield of photosystem II of the 17 DAP plumule between the two NILs, measured at light-adapted state. Data represents mean expression  $\pm$ SE; \*,  $P < 0.05$ ; \*\*,  $P < 0.01$ ; n.s., not significant (one-way ANOVA).

promoter of both maize embryos and leaves. The effects on embryos is considerably larger (Table S3 in Supporting Information), suggesting that the TE insertion led to different consequences for DNA methylation in embryos and leaves, which may also result from the microenvironments of different tissues.

Even more fascinating was the diel pattern of *ZmPORB1* expression in a B73 leaf during one day when light was switched on or off to simulate the sunrise at 6:00 and sunset at 18:00 (Figure S8D in Supporting Information). *ZmPORB1* expression was notably promoted 20 min after being exposed to light and 30 min after turning off the light, which infers that the light and oxygen response of *ZmPORB1* may function during the diel cycle as well as in order to adapt to the ambient environment. In conclusion, these data provided new insights in the transcriptional regulation of *ZmPORB1* in diverse tissues.

### Whilst long-neglected photosynthesis of the maize embryo appears to occur and to be physiologically relevant

In our study, we discovered that *ZmPORB1* affected chlorophyll content in the embryos, but not in leaves, while its homologous gene *ZmPORB2* controlled chlorophyll content in leaves. The development of the *porb2* single mutants with etiolated leaves was delayed by several days, while the *porb1/porb2* double mutants were characterized by more substantially decreased chlorophyll in leaves and heavily impeded plant growth, indicating that chlorophyll shortage may restrict photosynthesis

and thereby hamper metabolism. As such we conclude that these two genes have essential roles in chlorophyll synthesis and plant development. We also found that the other genes of chlorophyll biosynthesis had relatively high expression, providing further evidence that chlorophyll biosynthesis occurs in maize embryos (Dataset S3 in Supporting Information).

It has long been thought that the maize embryo is non-green and non-photosynthetic (Diepenbrock et al., 2017; Felker et al., 1995; Hunter et al., 2018; Magnard et al., 2004; Radchuk and Borisjuk, 2014), that oxygen levels are only determined by passive diffusion from the atmosphere (Borisjuk and Rolletschek, 2009), and thus that the embryo undergoes severe hypoxic stress during seed development. However, it was reported the oxygen concentration in internal embryo remained considerably higher ( $13.5\% \pm 6.5\%$ ) compared with that in the maize endosperm where it was negligible (Borisjuk and Rolletschek, 2009; Rolletschek et al., 2005). Oxygen is indispensable for ATP production through mitochondrial respiration, but excess oxygen also forms a high level of reactive oxygen species harmful to cells especially in the tissues with high physiological activities, hence, the oxygen level must be strictly regulated. Furthermore, we confirmed that the maize embryo is photosynthetically active and revealed that controlling the chlorophyll content via the regulation of *ZmPORB1* expression under light and oxygen cues represents a route to modulate the photosynthetic activity (Figure 5). We hope that we will be able to quantitatively determine the oxygen levels released by photosynthesis in maize

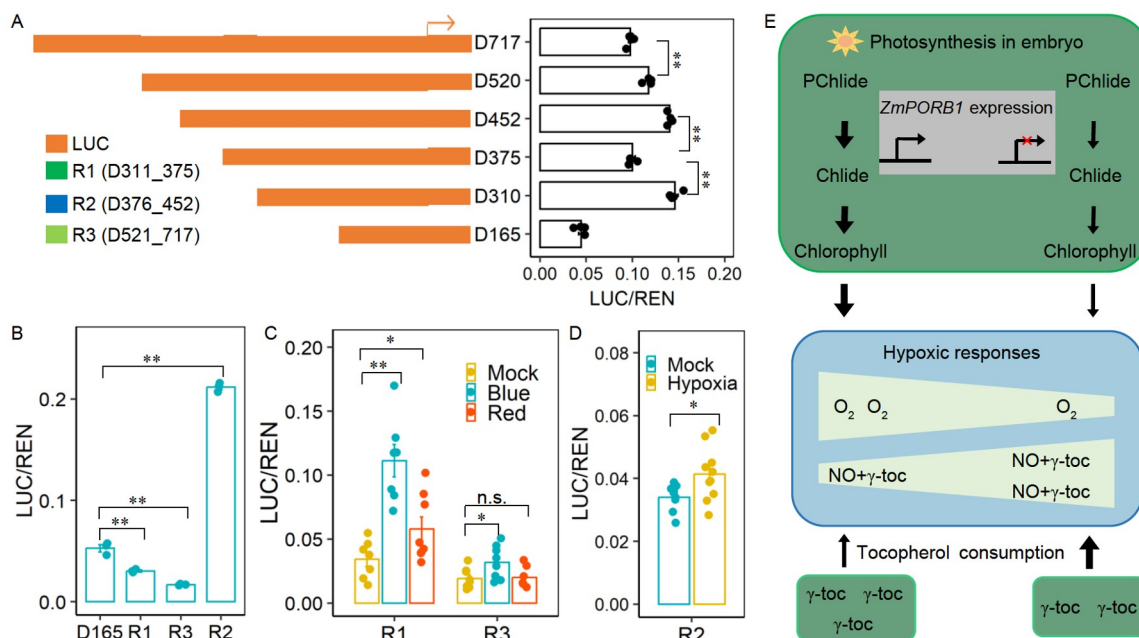


**Figure 6.** The promoter *cis*-elements for light and hypoxic responses of *ZmPORB1*. A, Schematic diagrams of truncated *ZmPORB1* promoter constructs and the corresponding LUC activity assays in maize protoplasts carrying different truncations by transient transformation. The letter “D” means the promoter fragments from NIL-DAN340, and the subsequent number represents the position upstream from the translation initiation site (ATG). B, The LUC activity assays in maize protoplasts for promoter fragments having an enhanced or suppressed effect on expression. The green bar graphs showed the enhanced or suppressed promoter fragments (D311\_375, D376\_452, D521\_717) jointed with the minimal promoter D165 which is the untranslated region. C, The LUC activity assays in tobacco leaves carrying the transient transformation of the promoter fragments (D311\_375, D521\_717) under dark, blue and red light. D, The LUC activity assays in maize protoplasts carrying the transient transformation of the promoter fragments (D376\_452) under hypoxia treatment. E, The model graph describing how *ZmPORB1* is involved in hypoxic and light responses to affect chlorophyll, NO, and  $\gamma$ -tocopherol levels in the developing maize embryos. During kernel development, *ZmPORB1* expression is regulated by incident light approaching the embryo surface and low oxygen, and further affects chlorophyll synthesis, which potentially takes part in photosynthesis and influences oxygen release to relieve the extreme oxygen deprivation observed in this tissue. Meanwhile,  $\gamma$ -tocopherol reacts to the promoted NO responding to hypoxia, which leads to its consumption and content variation. The greater the width of black array, the higher flux of metabolic and response pathway. The red cross means that *ZmPORB1* expression is destroyed and decreased. Data represents mean expression $\pm$ SE; \*,  $P<0.05$ ; \*\*,  $P<0.01$ ; n.s., not significant (one-way ANOVA).

embryos in our further studies. In conclusion, we propose the photosynthesis of embryo containing chlorophyll supplies oxygen essential for its metabolism. Our findings thus shed light on the mechanism for fine-tuning endogenous oxygen concentration through a novel and feedback pathway acting via the regulation of *ZmPORB1* expression and chlorophyll content by light and low oxygen in maize embryo.

It has been reported that non-leaf photosynthesis had some tissue-specific and adaptative mechanisms. In soybean, about 10% of incident light approached the embryo surface, and the oxygen produced by photosynthesis within embryo was affected by light intensity and quality (Borisjuk and Rolletschek, 2009). Embryonic photosynthesis may mostly provide oxygen to prevent anoxia and energy depletion instead of the accumulation of photoassimilates like achieved in leaves or is adapted for some particular pathway like the biosynthesis of oil storage in developing oilseed rape (*Brassica napus* L.) (Puthur et al., 2013; Schwender et al., 2004). Our results thus make an important contribution to our understanding of embryo photosynthesis of maize and the transcriptional regulation of oxygen levels. Such reports remind us that the chlorophyll content of non-leaf tissues should be quantified even in cases in which it is not visible to the naked eye, and highlight that non-leaf photosynthesis deserves considerably more research attention in the future.

The developing maize embryos are under low oxygen, and the regulation of NO levels is a core adaptive response for hypoxia. Decreases in endogenous oxygen concentrations will enhance

endogenous NO levels, while by contrast raising oxygen levels strongly lowers NO levels (Borisjuk et al., 2007). Meanwhile,  $\gamma$ -tocopherol is specialized in quenching reactive nitrogen species in order to protect the major components of the cell membrane from oxidation (Blokina and Fagerstedt, 2010). Here we found that NO levels were higher and the  $\gamma$ -tocopherol content lower in the embryos of NIL-K22. Referring to research suggesting that decreasing oxygen or  $H_2O_2$  had the same effects in hypoxic maize anther tissue (Kelliher and Walbot, 2012), we treated the developing maize kernels with NO and  $H_2O_2$  to simulate hypoxia and oxygen replenishment in our study, respectively. We observed that  $\gamma$ -tocopherol remarkably decreased when treated with NO and increased when treated with  $H_2O_2$ , indirectly indicating that  $\gamma$ -tocopherol participated in the response to hypoxia and that increasing oxygen resulted in the increasing of  $\gamma$ -tocopherol, and relieved the hypoxic stress in maize embryos. Our results thus provide new insights into the role of  $\gamma$ -tocopherol in hypoxia regulation, and may explain the curiosity as to why  $\gamma$ -tocopherol is mainly stored in maize embryos.

## MATERIALS AND METHODS

### QTL mapping and fine mapping of *qVE1*

192 lines of the recombinant inbred line (RIL) population DAN340/K22 (Pan et al., 2016) were planted in two trials in Yunnan and Chongqing (China) in 2011. The mature kernels

bulk from five plants of each line were collected for measuring the content of three forms of tocopherol ( $\delta$ -,  $\alpha$ -,  $\gamma$ -tocopherol). The methods used for tocopherol extraction were as in [Chander et al. \(2008\)](#), and quantification was performed by ultra performance liquid chromatography (UPLC, Waters, USA) using a BEH C18 column (2.1 mm $\times$ 100 mm, 1.7  $\mu$ m), the mobile phase was 25% methanol and 75% acetonitrile, with traces of butylated hydroxytoluene (BHT) and trimethylamine. The data from the two locations were analyzed using the linear mixed model that fitted genotypes and environment effects as random effect in the R package “lme4” ([R Core Team, 2012](#)). The BLUP values were used as the phenotypes in QTL analysis. Whole genome QTL mapping was conducted by WinQTLCart version 2.5 ([Wang et al., 2005](#)), the LOD cutoff was determined by 500 permutations, and the confidence interval was defined by the markers on both sides of the top LOD differing by 2 LOD.

Fine mapping in heterogeneous inbred families (HIF): 11 markers were developed in the  $\sim$ 2.3 Mb confidence interval (Table S4 in Supporting Information), one inbred line named HIF1 derived from the previously described HIF library ([Liu et al., 2018](#)) that were heterozygous in *qVE1* and homozygous in most of the rest of genome was chosen to validate this QTL by means of progeny tests, and was then used to develop large HIFs and five types of recombinants were identified among more than 10,000 lines. The genotypes of segregating families derived by selfing from these recombinants were determined using 11 segregating markers (Table S4 in Supporting Information) and the content of two tocopherol components in kernels were measured in the progeny. ANOVA of the three traits including  $\alpha$ -,  $\gamma$ - and total tocopherol was computed within each family between the two segregating genotypes corresponding to alleles from K22 and DAN340. The linkage map for the QTL region was constructed based on newly developed markers in MapMaker ([Lander et al., 2009](#)).

### BAC screening of K22 and ANOVA analysis to identify the causal variations for tocopherol

Three markers, M6, M8, within the candidate gene *ZmPORB1*, and M10 were used to screen the K22 BAC library by PCR, and the positive clones were sequenced by PacBio sequencing system. About 60 kb sequence mapped well to the reference genome B73 (RefGen\_V2) but some large structural variations were also found. By sequencing from 2 kb upstream of the 5'-UTR to the 3'-UTR of *ZmPORB1* in DAN340, we identified 59 SNPs and 15 InDels between the two parents DAN340 and K22 (Dataset S4 in Supporting Information). To identify the functional variations, we employed three PCR markers corresponding to the three transposons, 13.7 kb ( $-1,116$  bp away from TSS), 1.7 kb (2,891 bp TSS), and 6.7 kb (3,091 bp TSS), to screen inbred lines of AMP ([Yang et al., 2011](#)). In addition, two regions spanning about 1 kb in promoter and 730 bp in 3'-UTR of *ZmPORB1* were re-sequenced (primers 55P8-20 and 455gap3) in a subset of AMP. In all, 383 lines in promoter and 281 lines in 3'-UTR were sequenced and were aligned by Bioedit (Hall, 1999). Three InDel markers (P384-12, P384-14, UTR3-3) were developed within the structural variation in K22 and DAN340 and used to genotype AMP ( $N=520$ ). Combining the 29 markers within *ZmPORB1* from RNA-seq of 368 lines subset of AMP ([Fu et al., 2013](#)), totally 214 polymorphic sites spanning  $\sim$ 1 kb upstream of transcription start sites of *ZmPORB1* to 3'-UTR were

obtained. ANOVA analysis for 438 lines in AMP, omitting 35 high oil lines, was conducted to identify the markers that affect the tocopherol variation in maize grain.

### *ZmPORB1* expression analysis and RNA-seq

Four tissues, namely embryo, endosperm, whole kernel at 10, 15, 25 and 30 DAP, and mature ear leaf, were collected and total RNA was extracted in at least three biological repeats using Quick RNA isolation Kit (Huayueyang, Beijing, China). The reverse transcription of RNA into cDNA was performed using a cDNA Synthesis kit (TransGen Biotech, Beijing, China). The gene expression level in each sample was quantified by qPCR performed by Bio-Rad CFX96 real-time system (Bio-Rad, USA) with three technical replications. *ZmActin* (GRMZM2G126010) was an internal control and the  $2^{-\Delta\Delta C_t}$  method was used for normalization.

Since *ZmPORB1* was differently expressed between developing embryos of the two NILs, three samples of embryos at 10, 15 and 25 DAP from each genotype were collected for RNA-seq. The 150-bp paired-end Illumina hi-sequencing was conducted at the National Key Laboratory of Crop Genetic Improvement (Wuhan). An average of 6 gigabases of raw data were generated for each sample, TopHat-2.1.0 was used in alignment of the sequencing reads to the reference genome B73 (B73 RefGen\_v3), a total of 29,552 genes were identified. The gene expression was calculated and normalized using Deseq ([Anders and Huber, 2010](#)), and if the gene expression fold change between the NILs was larger than 1.5 and adjusted  $P$ -value $<0.05$ , then the gene was regarded as differential expression between NIL-K22 and NIL-DAN340. GO enrichment of DEGs was analyzed by The Gene Ontology Resource (<http://geneontology.org/>).

### Generation and characterization of overexpression and knockout lines of *ZmPORB1*

The full-length DNA sequence from start codon to stop codon of *ZmPORB1* amplified from the maize inbred line B73 and driven by a maize ubiquitin promoter was inserted into the over-expression vector pZZ-EGFP containing the *bar* marker gene. The resulting plasmids Ubi::*ZmPORB1* were transferred into maize inbred line KN5585, and the positive plants containing *bar* gene were selected according to the herbicide resistance in  $T_0$ . The two positive transgenic plants named OE1, OE2 were planted into  $T_3$  families under normal conditions in Huazhong Agriculture University trial field in 2017, plants of the two families were detected by bar test strip to detect positive and negative lines (Envirologix, USA) and the target gene *ZmPORB1* expression of embryo in each line was tested by qPCR using a pair of primers named 55qp-1. The  $\alpha$ -tocopherol and  $\gamma$ -tocopherol levels were subsequently measured in mature kernels of the two families including positive and negative plants.

Considering that the weak mutations of *ZmPORB1* exhibit significant phenotype difference under the background of weak mutations in *ZmPORB2*, we analyzed the allele of *ZmPORB2* in the maize inbred line KN5585, and found the 5 kb sequence of promoter have 99% identities with that of the parents K22, both of them have little *ZmPORB2* expression in embryo (unpublished RNA-seq data), which means *ZmPORB2* shows weak mutation in the inbred line KN5585 (Dataset S5 in Supporting Information). To obtain knockout lines of *ZmPORB1*, *ZmPORB2*, we designed

one and two guide RNA to edit the second and third exon, respectively. The gRNAs of each gene were cloned into a CRISPR/Cas9 plant expression vector (Liu et al., 2020) and transformed into KN5585 by Agrobacterium-mediated transformation at WIMI Biotechnology Co., Ltd. (Changzhou, China). The gRNA of *ZmPORB1* is GAAGACCCTCCGCAAGGGCACGG; the two gRNAs of *ZmPORB2* are GACCCTCCGCAAGGGCACGG and GGTGTTCTGCTCGCGCGGA. The primers (Table S4 in Supporting Information) were used to detect the genotype of *zmporb1* and *zmporb2* mutants in order to detect the sequence variations by Sanger sequencing.

### Light and hypoxia treatment of leaves and kernels of NIL-DAN340 and NIL-K22

For light and hypoxia treatment of 15 DAP kernels, at least 180 kernels of the two NILs from three biological repetitions were intactly fallen off from cobs and split into two groups each with three copies, respectively. One group was placed in three conditions, red, blue light and dark for eight hours at room temperature, and the other group was treated under hypoxia and anaerobic condition in two hypoxia containers (7L, C31, MGC) with one or two oxygen-consumption bags (3.5 L AnaeroPack, MGC, Japan) for four hours in dark, the control was under normal atmosphere in dark. Thirty kernels of each treatment of the two NILs were frozen by liquid nitrogen and grounded into powders to detect *ZmPORB1* expression. For light treatment of leaves of two NILs, the leaves continuously growing under dark for six days were moved to red, blue light for four hours, and at least six biological repetitions were collected to detect *ZmPORB1* expression. And the total RNA from three hypoxia-treated kernels and three controls was sequenced of NIL-DAN340 in order to uncover the DEGs.

### Sub-cellular localization of ZmPORB1

In order to determine ZmPORB1 subcellular localization, we amplified the coding sequence of *ZmPORB1* using the cDNA of B73 as a template with primers designed specifically for *ZmPORB1*. The PCR product was inserted into the pM999-GFP vector which was digested with *Xba*I. To construct an ORF encoding a GFP fused protein driven by the 35S promoter, we isolated maize protoplasts as described (Yoo et al., 2007) and transformed them with the pM999-35S-ZmPORB1-GFP vector using a PEG-calcium-mediated method. Transformed protoplasts were cultured at 23°C in the dark overnight. Fluorescence in the transformed protoplasts was imaged using a confocal laser scanning microscope (FV1200, Olympus, Japan).

### Phylogenetic analysis and expression profile analysis

Protein sequences, cDNA sequences and the corresponding data of gene expression homologous with *ZmPORB1* were downloaded from maize (*GRMZM2G073351*, *GRMZM2G084958*) (<http://www.gramene.org/>), rice (*Os10g0496900*, *Os04T0678700*) (<http://rice.plantbiology.msu.edu/index.shtml>), sorghum (*SORBI\_001G206200*, *SORBI\_006G268200*), *Brachypodium* (*BRADI3G57380*, *BRADI5G26230*) (Gramene, <http://www.gramene.org/>) and *Arabidopsis* (*AT1G03630*, *AT5G54190*, *AT4G27440*) (<http://www.arabidopsis.org/>), all protein sequences were aligned by CLUSTALW (<http://www.genome.jp/tools/clustalw/>).

These proteins were used to construct a phylogenetic tree using the maximum likelihood method based on MEGA5 (Tamura et al., 2011).

### Extraction and determination of chlorophyll, HGA and PMP

Two forms of chlorophyll, chlorophyll a and b, were extracted from 15 DAP embryos of knockout lines of *zmporb1-1*. The embryos were freeze dried and ground into powder, and extracting methods referred to Diepenbrock et al. (2017). Chlorophyll was detected by LC-MS/MS (multiple-reaction-monitoring mode) with a mass spectrometer QTRAP 4000 (AB Sciex, Canada) mass spectrometer coupled to a liquid chromatography system (LC20A HPLC, Shimadzu, Japan) (Jouhet et al., 2017). Analyses were achieved in positive mode. Chlorophyll was separated on an Accucore C30 (100 mm×2.1 mm, particle size, 2.6 μm, Waters) using Eluent A and B solutions. Eluent A was formula water:methanol:acetonitrile:300 mmol L<sup>-1</sup> ammonium acetate=20:20:20:1 (v/v/v/v), and eluent B was isopropanol:methanol:300 mmol L<sup>-1</sup> ammonium acetate=180:20:3 (v/v/v). The gradient elution program was as follows: 0–2 min, 25%–40% eluent B; 2–4 min, 40%–95% eluent B; and 4–18 min, eluent 95% B. The flow rate was 0.3 mL min<sup>-1</sup>. The areas of LC peaks were determined using MultiQuant software (AB Sciex) for relative quantification (Zhao et al., 2022). And the extraction and determination methods of leaves chlorophyll were referred to Arnon (1949). About 0.2 g of fresh mature leaves above ear of knockout lines of *zmporb1-1*, *zmporb1-2*, *zmporb2*, *zmporb1-2/zmporb2* (the top leaves) were collected to be soaked in 8 mL 95% ethanol by shaking until the green fading in the dark, and the contents were measured by MicroplateReader. The chlorophyll a and chlorophyll b standards were purchased from Sigma-Aldrich (USA).

The precursors HGA and PMP were extracted from mature kernels and developing kernels at 25, 30 and 35 DAP of the two NILs. HGA and Phytyl Monophosphate-DA standards were bought from Sigma-Aldrich and Larodan (Sweden), respectively. The kernels were freeze dried and ground into powder, and 100 mg of the powder of these samples were extracted by adding a mixture of isopropanol, formic acid and water, then let them stand for 20 min and ultrasonicated for 30 min at low temperature; and chloroform was added into the mixture, which was subject to another round of ultrasonication. Next, after vortex for 1 min, the mixture was centrifugated at 13,000×g for 5 min, and the lower organic phase was obtained, subsequently evaporated and re-dissolved in 50% methanol. HGA and PMP were quantified by Liquid Chromatography-Mass Spectrometry including UPLC (Waters) using a BEH C18 column (2.1 mm×100 mm, 1.7 μm) and triple quadrupole mass spectrometer with JetStream ESI source (AB Sciex), the method was modified based on the study of vom Dorp et al. (2015). The mobile phase was a gradient of acetonitrile and 5 mmol L<sup>-1</sup> aqueous ammonium acetate, and the concentration of acetonitrile increased to 90% in 5 min.

### The assay of NO and H<sub>2</sub>O<sub>2</sub> content of maize embryos

The embryos of two NILs were entirely peeled off from 15 DAP kernel with at least ten biological repetitions, and were placed in a buffer (5 mmol L<sup>-1</sup> 2-(N-morpholino) ethanesulfonic acid

(MES), pH 5.7, 1 mmol L<sup>-1</sup> CaCl<sub>2</sub>, 0.25 mmol L<sup>-1</sup> KCl) with or without 400 μmol L<sup>-1</sup> cPTIO for 1 h. Then the buffer was removed prior to the addition of 20 μmol L<sup>-1</sup> DAF-FMDA for 30 min, and washed in loading buffer for 30 min. The fluorescence of embryo was monitored by a fluorescence microscope (Nikon, Japan). The samples treated with cPTIO were the negative control to report autofluorescence levels, and the fluorescence of all samples was quantified using ImageJ (Vishwakarma et al., 2019).

200–300 mg powder (fresh weight) of 25 DAP kernels of two NILs from at least three biological repetitions were used to detect the H<sub>2</sub>O<sub>2</sub> content by Hydrogen Peroxide (H<sub>2</sub>O<sub>2</sub>) Content Assay Kit (Micromethod, Sangon Biotech, Shanghai, China). In addition, 15 DAP embryos from four biological repetitions were peeled off from the kernels, and dipped into 10 μmol L<sup>-1</sup> H<sub>2</sub>DCFDA (Invitrogen, USA) for 2 h in the dark prior to resin with double distilled water (Kaur et al., 2016). Finally, the fluorescence of embryo was monitored by a fluorescence microscope (Nikon).

### γ-tocopherol content under NO and H<sub>2</sub>O<sub>2</sub> treatment

25 DAP kernels of the two NILs were intactly peeled off from 5 cobs, totally about 70 kernels were incubated in each plate with a series of gradients of NO donor (sodium nitroprusside, 0, 0.05, 0.1 mmol L<sup>-1</sup>), similarly, the kernels were incubated with a series of gradients of H<sub>2</sub>O<sub>2</sub> (0, 5, 10 mmol L<sup>-1</sup>) for 40 h. Then, the kernels from each treatment with at least 15 biological repetitions were frozen dried and ground into powder for detection of γ-tocopherol.

### Chlorophyll Fluorescence Imaging

Maize kernels of the two NILs at 17 DAP were adapted to the dark for 20 min, then under these dark conditions the embryos were peeled and sliced through their centres under dark. Estimates of key chlorophyll fluorescence parameters were obtained using a Micro-FluorCam chlorophyll fluorometer (Micro-FluorCam FC 2000, PSI, Czech Republic) with 10× magnification allowing the minimum chlorophyll fluorescence of dark adaptation (F<sub>0</sub>) to be obtained. Subsequently, the embryos were re-illuminated with red light to achieve a steady state rate of photosynthesis, and actinic irradiances were imposed for 320 s in order to measure the steady state chlorophyll fluorescence (F<sub>t\_Lss</sub>), and the maximum fluorescence yield (F<sub>m\_Lss</sub>) was measured on exposure to saturating light intensity. Estimates of the effective quantum yield of PSII (QY\_Lss) were obtained from the digitized images of F<sub>t\_Lss</sub> and F<sub>m\_Lss</sub> by a pixel-by-pixel calculation of [(F<sub>m\_Lss</sub>–F<sub>t\_Lss</sub>)/F<sub>m\_Lss</sub>].

### The dual-luciferase reporter assay to detect the light and hypoxia responsive elements of *ZmPORB1*

In order to explore which regions of promoter that light and hypoxia responsive elements located in, firstly, we checked whether the 13.7 kb TE insertion destroyed the key *cis*-elements, and we compared the activity of 1.5 kb, 1.25 kb of DAN340 allele and 1.25 kb of K22 allele of *ZmPORB1* by dual-luciferase reporter assay in maize protoplasts. The promoter start site of *ZmPORB1* was regarded as the upstream of the ATG start codon. Secondly, we separated the upstream 1.25 kb of DAN340 allele

from start site into 165 bp (D165, 5'-UTR), 254 bp (D254), 310 bp (D310), 375 bp (D375), 452 bp (D452), 520 bp (D520), 717 bp (D717), 1,250 bp (D1250) to detect the transcriptional activity in maize protoplasts. Thirdly, according to the transcriptional effects of above-mentioned truncated regions, we identified the suppressive (D311\_375, D521\_717, D255\_310, D718\_1250) and activated (D376\_452) fragments, which were subsequently joined with the minimal promoter D165 to verified the positive or negative effects in maize protoplasts. Fourthly, the promoter fragments, D311\_375 (R1) and D521\_717 (R2), were used to examine the response of red and light in tobacco by transient expression of dual-luciferase reporter assay. The D376\_452 (R2) was used to examine the response of hypoxia in maize protoplasts under hypoxic treatment.

All the above-mentioned promoter fragments were jointed with pGreen II 0800-LUC binary vector. The maize protoplast isolation and transfection were referred to Yoo et al. (2007). For tobacco (*Nicotiana benthamiana*), *Agrobacterium* cells harboring the pGreen II 0800-LUC recombinant vector and the help vector pSoup were injected into young tobacco leaves that were one month old, after that, the plants were exposed to red, blue and dark condition for 72 h, and the LUC and Ren activity were measured with a Dual-Luciferase® Reporter Assay System (Promega, USA) by MicroplateReader, each transformation event has six biological repetitions. For hypoxia treatment of maize protoplasts, the protoplasts transfected with the D376\_452-LUC vector incubated in the dark for 12 h, then half of the samples were transferred to the hypoxia container (7L, C31, MGC) with two oxygen-consumption bags (3.5 L AnaeroPack, MGC) for 5 h, and the LUC and Ren activity were measured.

### Bisulphite analysis

~500 ng of genomic DNA from embryos at 15 DAP and mature leaves of two NILs were treated using EZ DNA Methylation-Lightning Kit (Zymo Research, USA), each sample has four biological repetitions. After bisulphite conversion, the treated DNA was amplified by PCR using KAPA HiFi HotStart Uracil ReadyMix Kit (Roche, Switzerland), and the PCR products were sequenced by next-generation sequencing. We utilized 4 pairs of primers to obtain the sequences of about 1.2 kb promoter of *ZmPORB1* (Table S4 in Supporting Information). The methylation levels were analyzed by bsmap (Xi and Li, 2009).

### Accession numbers

*ZmPORB1*: GRMZM2G036455, *ZmPORB2*: GRMZM2G073351; *ZmPORA*: GRMZM2G084958; *OsPORB*: Os10g0496900, *OsPORA*: Os04T0678700; *SbPOR1*: SORBI\_001G206200; *SbPOR2*: SORBI\_006G268200; *BdPOR1*: BRADI3G57380; *BdPOR2*: BRADI5G26230; *AtPORC*: AT1G03630; *AtPORA*: AT5G54190; *AtPORB*: AT4G27440.

### Compliance and ethics

The author(s) declare that they have no conflict of interest.

### Acknowledgement

This work was supported by the National Natural Science Foundation of China (32200221, U1901201), the National Key Research and Development Program of China (2022YFD1201502), the Key Area Research and Development Program of Guangdong Province, China (2022B0202060003), and Huazhong Agricultural University Scientific & Technological Self-Innovation Foundation. We thank Dr. Bailin Li from DuPont-Pioneer for helping to construct the BAC library of K22 and sequence the target BAC.

## Supporting information

The supporting information is available online at <https://doi.org/10.1007/s11427-023-2489-2>. The supporting materials are published as submitted, without typesetting or editing. The responsibility for scientific accuracy and content remains entirely with the authors.

## References

- Abbasi, A.R., Hajirezaei, M., Hofius, D., Sonnewald, U., and Voll, L.M. (2007). Specific roles of  $\alpha$ - and  $\gamma$ -tocopherol in abiotic stress responses of transgenic tobacco. *Plant Physiol* 143, 1720–1738.
- Albert, E., Kim, S., Magallanes-Lundback, M., Bao, Y., Deason, N., Danilo, B., Wu, D., Li, X., Wood, J.C., Bornowski, N., et al. (2022). Genome-wide association identifies a missing hydrolase for tocopherol synthesis in plants. *Proc Natl Acad Sci USA* 119, e2113488119.
- Anders, S., and Huber, W. (2010). Differential expression analysis for sequence count data. *Genome Biol* 11, R106.
- Arnon, D. (1949). Copper enzymes isolated chloroplasts, polyphenoloxidase in *Beta vulgaris*. *Plant Physiol* 24, 1–15.
- Blokhina, O., and Fagerstedt, K.V. (2010). Oxidative metabolism, ROS and NO under oxygen deprivation. *Plant Physiol Biochem* 48, 359–373.
- Borisjuk, L., Macherel, D., Benamar, A., Wobus, U., and Rolletschek, H. (2007). Low oxygen sensing and balancing in plant seeds: a role for nitric oxide. *New Phytol* 176, 813–823.
- Borisjuk, L., and Rolletschek, H. (2009). The oxygen status of the developing seed. *New Phytol* 182, 17–30.
- Chander, S., Guo, Y.Q., Yang, X.H., Yan, J.B., Zhang, Y.R., Song, T.M., and Li, J.S. (2008). Genetic dissection of tocopherol content and composition in maize grain using quantitative trait loci analysis and the candidate gene approach. *Mol Breed* 22, 353–365.
- Christen, S., Woodall, A.A., Shigenaga, M.K., Southwell-Keely, P.T., Duncan, M.W., and Ames, B.N. (1997).  $\gamma$ -Tocopherol traps mutagenic electrophiles such as  $\text{NO}_x$  and complements  $\alpha$ -tocopherol: Physiological implications. *Proc Natl Acad Sci USA* 94, 3217–3222.
- Collakova, E., and DellaPenna, D. (2003). The role of homogentisate phytyltransferase and other tocopherol pathway enzymes in the regulation of tocopherol synthesis during abiotic stress. *Plant Physiol* 133, 930–940.
- Cooney, R.V., Franke, A.A., Harwood, P.J., Hatch-Pigott, V., Custer, L.J., and Mordan, L.J. (1993). Gamma-tocopherol detoxification of nitrogen dioxide: superiority to alpha-tocopherol. *Proc Natl Acad Sci USA* 90, 1771–1775.
- Desel, C., Hubermann, E.M., Schwarz, K., and Krupinska, K. (2007). Nitration of  $\gamma$ -tocopherol in plant tissues. *Planta* 226, 1311–1322.
- Desel, C., and Krupinska, K. (2005). The impact of tocopherols on early seedling development and NO release. *J Plant Physiol* 162, 771–776.
- Diepenbrock, C.H., Kandianis, C.B., Lipka, A.E., Magallanes-Lundback, M., Vaillancourt, B., Góngora-Castillo, E., Wallace, J.G., Cepela, J., Mesberg, A., Bradbury, P.J., et al. (2017). Novel loci underlie natural variation in vitamin E levels in maize grain. *Plant Cell* 29, 2374–2392.
- Felker, F.C., Doehlert, D.C., and Eskins, K. (1995). Effects of red and blue light on the composition and morphology of maize kernels grown *in vitro*. *Plant Cell Tiss Organ Cult* 42, 147–152.
- Fiedler, E., Soll, J., and Schultz, G. (1982). The formation of homogentisate in the biosynthesis of tocopherol and plastoquinone in spinach chloroplasts. *Planta* 155, 511–515.
- Fitzpatrick, T.B., Basset, G.J.C., Borel, P., Carrari, F., DellaPenna, D., Fraser, P.D., Hellmann, H., Osorio, S., Rothan, C., Valpuesta, V., et al. (2012). Vitamin deficiencies in humans: can plant science help? *Plant Cell* 24, 395–414.
- Fritsche, S., Wang, X., and Jung, C. (2017). Recent advances in our understanding of tocopherol biosynthesis in plants: an overview of key genes, functions, and breeding of vitamin E improved crops. *Antioxidants* 6, 99.
- Fu, J., Cheng, Y., Linghu, J., Yang, X., Kang, L., Zhang, Z., Zhang, J., He, C., Du, X., Peng, Z., et al. (2013). RNA sequencing reveals the complex regulatory network in the maize kernel. *Nat Commun* 4, 2832.
- Geigenberger, P. (2003). Response of plant metabolism to too little oxygen. *Curr Opin Plant Biol* 6, 247–256.
- Hall, T.A. (1999). BioEdit: a user-friendly biological sequence alignment editor a analysis program for Windows 95/98/NT. *Nucleic Acids Symp*, 95–98.
- Horvath, G., Wessjohann, L., Bigirimana, J., Jansen, M., Guisez, Y., Caubergs, R., and Horemans, N. (2006). Differential distribution of tocopherols and tocotrienols in photosynthetic and non-photosynthetic tissues. *Phytochemistry* 67, 1185–1195.
- Hunter, C.T., Saunders, J.W., Magallanes-Lundback, M., Christensen, S.A., Willett, D., Stinard, P.S., Li, Q., Lee, K., DellaPenna, D., and Koch, K.E. (2018). Maize *w3* disrupts *homogentisate solanessyl transferase* (*ZmHst*) and reveals a plastoquinone-9 independent path for phytoene desaturation and tocopherol accumulation in kernels. *Plant J* 93, 799–813.
- Jouhet, J., Lupette, J., Clerc, O., Magneschi, L., Bedhomme, M., Collin, S., Roy, S., Maréchal, E., and Rébeillé, F. (2017). LC-MS/MS versus TLC plus GC methods: Consistency of glycerolipid and fatty acid profiles in microalgae and higher plant cells and effect of a nitrogen starvation. *PLoS ONE* 12, e0182423.
- Kaur, N., Sharma, I., Kirat, K., and Pati, P. (2016). Detection of reactive oxygen species in *Oryza sativa* L. (rice). *Bio-Protocol* 6, e2061.
- Kelliher, T., and Walbot, V. (2012). Hypoxia triggers meiotic fate acquisition in maize. *Science* 337, 345–348.
- Klinkenberg, J., Faist, H., Saupe, S., Lambert, S., Kriskchke, M., Stingl, N., Fekete, A., Mueller, M.J., Feussner, I., Hedrich, R., et al. (2014). Two fatty acid desaturases, STEAROYL-ACYL CARRIER PROTEIN  $\Delta^9$ -DESATURASE6 and FATTY ACID DESATURASE3, are involved in drought and hypoxia stress signaling in *Arabidopsis* crown galls. *Plant Physiol* 164, 570–583.
- Lander, E.S., Green, P., Abrahamson, J., Barlow, A., Daly, M.J., Lincoln, S.E., and Newberg, L.A. (2009). Corrigendum to “MAPMAKER: An interactive computer package for constructing primary genetic linkage maps of experimental and natural populations” [Genomics 1 (1987) 174–181]. *Genomics* 93, 398.
- Liu, H.J., Jian, L., Xu, J., Zhang, Q., Zhang, M., Jin, M., Peng, Y., Yan, J., Han, B., Liu, J., et al. (2020). High-throughput CRISPR/Cas9 mutagenesis streamlines trait gene identification in maize. *Plant Cell* 32, 1397–1413.
- Liu, N., Liu, J., Li, W., Pan, Q., Liu, J., Yang, X., Yan, J., and Xiao, Y. (2018). Intraspecific variation of residual heterozygosity and its utility for quantitative genetic studies in maize. *BMC Plant Biol* 18, 66.
- Maeda, H., Sakuragi, Y., Bryant, D.A., and DellaPenna, D. (2005). Tocopherols protect *Synechocystis* sp. strain PCC 6803 from lipid peroxidation. *Plant Physiol* 138, 1422–1435.
- Maeda, H., Song, W., Sage, T.L., and DellaPenna, D. (2006). Tocopherols play a crucial role in low-temperature adaptation and phloem loading in *Arabidopsis*. *Plant Cell* 18, 2710–2732.
- Magnard, J.L., Heckel, T., Massonneau, A., Wisniewski, J.P., Cordelier, S., Lassagne, H., Perez, P., Dumas, C., and Rogowsky, P.M. (2004). Morphogenesis of maize embryos requires *ZmPRPL35-1* encoding a plastid ribosomal protein. *Plant Physiol* 134, 649–663.
- Mène-Saffrané, L., and DellaPenna, D. (2010). Biosynthesis, regulation and functions of tocopherols in plants. *Plant Physiol Biochem* 48, 301–309.
- Munné-Bosch, S. (2005). The role of alpha-tocopherol in plant stress tolerance. *J Plant Physiol* 162, 743–748.
- Mustroph, A., Lee, S.C., Oosumi, T., Zanetti, M.E., Yang, H., Ma, K., Yaghoubi-Masihi, A., Fukao, T., and Bailey-Serres, J. (2010). Cross-kingdom comparison of transcriptomic adjustments to low-oxygen stress highlights conserved and plant-specific responses. *Plant Physiol* 152, 1484–1500.
- Pan, Q., Li, L., Yang, X., Tong, H., Xu, S., Li, Z., Li, W., Muehlbauer, G.J., Li, J., and Yan, J. (2016). Genome-wide recombination dynamics are associated with phenotypic variation in maize. *New Phytol* 210, 1083–1094.
- Pucciariello, C., and Perata, P. (2017). New insights into reactive oxygen species and nitric oxide signalling under low oxygen in plants. *Plant Cell Environ* 40, 473–482.
- Puthur, J.T., Shackira, A.M., Saradhi, P.P., and Bartels, D. (2013). Chloroembryos: A unique photosynthesis system. *J Plant Physiol* 170, 1131–1138.
- R Core Team. (2012). R: a language and environment for statistical computing. Vienna: R Foundation for Statistical Computing. Available from URL: <http://www.R-project.org/>.
- Radchuk, V., and Borisjuk, L. (2014). Physical, metabolic and developmental functions of the seed coat. *Front Plant Sci* 5, 510.
- Rocheford, T.R., Wong, J.C., Egesel, C.O., and Lambert, R.J. (2002). Enhancement of vitamin E levels in corn. *J Am Coll Nutr* 21, 191S–198S.
- Rolletschek, H., Koch, K., Wobus, U., and Borisjuk, L. (2005). Positional cues for the starch/lipid balance in maize kernels and resource partitioning to the embryo. *Plant J* 42, 69–83.
- Sattler, S.E., Cahoon, E.B., Coughlan, S.J., and DellaPenna, D. (2003). Characterization of tocopherol cyclases from higher plants and Cyanobacteria. Evolutionary implications for tocopherol synthesis and function. *Plant Physiol* 132, 2184–2195.
- Sattler, S.E., Gilliland, L.U., Magallanes-Lundback, M., Pollard, M., and DellaPenna, D. (2004). Vitamin E is essential for seed longevity and for preventing lipid peroxidation during germination. *Plant Cell* 16, 1419–1432.
- Schwender, J., Goffman, F., Ohlrogge, J.B., and Shachar-Hill, Y. (2004). Rubisco without the Calvin cycle improves the carbon efficiency of developing green seeds. *Nature* 432, 779–782.
- Soll, J., Kemmerling, M., and Schultz, G. (1980). Tocopherol and plastoquinone synthesis in spinach chloroplasts subfractions. *Arch Biochem Biophys* 204, 544–550.
- Stahl, E., Hartmann, M., Scholten, N., and Zeier, J. (2019). A role for tocopherol biosynthesis in *Arabidopsis* basal immunity to bacterial infection. *Plant Physiol* 181, 1008–1028.
- Tamura, K., Peterson, D., Peterson, N., Stecher, G., Nei, M., and Kumar, S. (2011). MEGA5: molecular evolutionary genetics analysis using maximum likelihood,

- evolutionary distance, and maximum parsimony methods. *Mol Biol Evol* 28, 2731–2739.
- Valentin, H.E., Lincoln, K., Moshiri, F., Jensen, P.K., Qi, Q., Venkatesh, T.V., Karunanandaa, B., Baszis, S.R., Norris, S.R., Savidge, B., et al. (2006). The *Arabidopsis vitamin E pathway gene5-1* mutant reveals a critical role for phytol kinase in seed tocopherol biosynthesis. *Plant Cell* 18, 212–224.
- van Dongen, J.T., and Licausi, F. (2015). Oxygen sensing and signaling. *Annu Rev Plant Biol* 66, 345–367.
- Vishwakarma, A., Wany, A., Pandey, S., Bulle, M., Kumari, A., Kishorekumar, R., Igamberdiev, A.U., Mur, L.A.J., and Gupta, K.J. (2019). Current approaches to measure nitric oxide in plants. *J Exp Bot* 70, 4333–4343.
- vom Dorp, K., Hölzl, G., Plohmman, C., Eisenhut, M., Abraham, M., Weber, A.P.M., Hanson, A.D., and Dörmann, P. (2015). Remobilization of phytol from chlorophyll degradation is essential for tocopherol synthesis and growth of *Arabidopsis*. *Plant Cell* 27, 2846–2859.
- Walley, J.W., Sartor, R.C., Shen, Z., Schmitz, R.J., Wu, K.J., Urlich, M.A., Nery, J.R., Smith, L.G., Schnable, J.C., Ecker, J.R., et al. (2016). Integration of omic networks in a developmental atlas of maize. *Science* 353, 814–818.
- Wang, S., Basten, C., and Zeng, Z. (2005). Windows QTL cartographer version 2.5. Statistical genetics. Raleigh: North Carolina State University.
- Weits, D.A., van Dongen, J.T., and Licausi, F. (2021). Molecular oxygen as a signaling component in plant development. *New Phytol* 229, 24–35.
- Xi, Y., and Li, W. (2009). BSMAP: whole genome bisulfite sequence MAPPING program. *BMC Bioinf* 10, 232.
- Yang, X., Gao, S., Xu, S., Zhang, Z., Prasanna, B.M., Li, L., Li, J., and Yan, J. (2011). Characterization of a global germplasm collection and its potential utilization for analysis of complex quantitative traits in maize. *Mol Breed* 28, 511–526.
- Yoo, S.D., Cho, Y.H., and Sheen, J. (2007). *Arabidopsis* mesophyll protoplasts: a versatile cell system for transient gene expression analysis. *Nat Protoc* 2, 1565–1572.
- Zhan, W., Liu, J., Pan, Q., Wang, H., Yan, S., Li, K., Deng, M., Li, W., Liu, N., Kong, Q., et al. (2019). An allele of *Zm<sup>PORB</sup> 2* encoding a protochlorophyllide oxidoreductase promotes tocopherol accumulation in both leaves and kernels of maize. *Plant J* 100, 114–127.
- Zhao, J., Sun, P., Sun, Q., Li, R., Qin, Z., Sha, G., Zhou, Y., Bi, R., Zhang, H., Zheng, L., et al. (2022). The MoPah1 phosphatidate phosphatase is involved in lipid metabolism, development, and pathogenesis in *Magnaporthe oryzae*. *Mol Plant Pathol* 23, 720–732.